Preprint typeset in JINST style - HYPER VERSION

arXiv:1403.4273v1 [physics.ins-det] 17 Mar 2014

Asymmetries in Silicon Microstrip Response Function and Lorentz Angle

Gregorio Landi[a*], **and Giovanni E. Landi**[b]

[a] *Dipartimento di Fisica e Astronomia, Universita' di Firenze,*
Largo E. Fermi 2 50125 Firenze Italy
and INFN, Sezione di Firenze,
Firenze,Italy
E-mail: landi@fi.infn.it

[b] *UBICA s.r.l.,*
Via S. Siro 6/1,
Genova, Italy.

ABSTRACT: An experimental set up, dedicated to isolate an error present in the η-algorithm, gave an unexpected result. The average of a center of gravity algorithm at orthogonal particle incidence turns out to be non zero. This non zero average signals an asymmetry in the response function of the strips, and introduces a further parameter in the corrections: the shift of the strip response center of gravity respect its geometrical position. A strategy to extract this parameter from a standard data set is discussed. Some simulations with various asymmetric response functions are explored for this test. The method is able to detect easily the asymmetry parameters introduced in the simulations. Its robustness is tested against angular rotations, and we see an almost linear variation with the angle. This simple property is used to simulate a determination of a Lorentz angle with and without the asymmetry of the response function.

KEYWORDS: Particle tracking detectors; Si microstrip and pad detectors; Data processing methods; Pattern recognition, cluster finding, calibration and fitting methods.

*Corresponding author.

Contents

1. Introduction **1**

2. Correction of the systematic errors **3**
- 2.1 COG averages 3
- 2.2 The η-Algorithms 5
- 2.3 Correction of the η Algorithms 6

3. Determination of δ_g **8**
- 3.1 Signal reconstruction 8
- 3.2 Generic Response Function 8
- 3.3 Inverse function of $\varepsilon_k(x_{gk})$ 8
- 3.4 Analytical form of $x_g(\varepsilon)$ 10
- 3.5 Simulations 12
- 3.6 Normal strips 15

4. Non orthogonal incidence and Lorentz angle **16**
- 4.1 Asymmetry due to non orthogonal incidence 16
- 4.2 Lorentz angle 18

5. Conclusions **21**

1. Introduction

In many high-energy physics experiments, arrays of silicon microstrip detectors are fundamental tools to track charged particles. The excellent position resolution of these detectors is essential in the event reconstruction. To obtain the best performance, the role played by the position-reconstruction algorithms becomes crucial. For example, the final alignments are corrected with track reconstructions; any inaccuracy in the position reconstruction algorithms is systematically diffused to all the data. The use of reconstruction algorithms in the detector alignment and in the data creates correlations that renders almost impossible to verify their consistency. Thus, an *a priori* exploration of their systematic errors is essential.

In a previous article [3] we applied to silicon microstrip detectors the general equations we developed in [1, 2] for the center of gravity (COG) algorithm. Among the many properties demonstrated for the COG, we underlined the presence of a systematic error in the so called η-algorithm [4], when used outside the symmetry conditions. The authors in [4] recommended the limitation to a symmetric configuration without demonstration. Thus, in the last years, the recommendation has

been neglected, and the η-algorithm has been used well outside its range of validity. It is easy to guess the production of many incorrect position reconstructions.

The η-algorithm improves the COG-algorithm with a global analysis of a set of equivalent data. Our procedure to define the $\eta-$algorithm is substantially different from that used in [4]. We deduce it from the solution of a first order differential equation that has an easy solution for a uniform distribution of impact points. But, any first order differential equation always requires an initial constant, in this case an exact impact point corresponding to a COG value. This type of datum is never available excluding some special cases. The initial constant is easily selected for symmetrical configurations, and is zero with the definitions of [4]. For unsymmetrical configuration, for example at non-orthogonal incidence angles, an angle dependent shift is produced by the use of the zero constant of the symmetric case. The shift depends on the form of the signal distribution. Thus, detectors aligned with minimum ionizing particles (MIP) could show non alignments with heavy ions (in reality there are non alignments in both cases). Similar apparent shift of a detector could be induced by the modification of the depleting tension or any other deformation of the signal distribution. Simulations show shifts greater than the root mean square (RMS) error in some directions, and always larger than the full width half maximum (FWHM) of the error distributions. In ref. [3], we demonstrate a method to correct it.

We have to underline the importance of the η-algorithm in improving the position reconstructions. The comparison of the RMS-error of the COG and η-algorithm does not show dramatic differences in favor of the latter, as the comparison of the FWHM. The reason of the small sensitivity of the RMS-error to the improvement of the η-algorithm is connected to the non-linear dependence of the two algorithms from their component stochastic variables. As it is well known, non-linearities introduce drastic deviation from the gaussian distributions toward slow decreasing probability distributions. The Cauchy distribution is a typical member of this class. These non-gaussian distributions tend to have infinite variances as the Cauchy distribution. In this case, the RMS-error is essentially limited the selection strategy of the finite sample and it is insensible to the quality of the reconstruction algorithms. On the contrary the FWHM saves its sensitivity.

In a test beam with a set of sensors of the PAMELA tracker [5], a special set up was exposed to the beam with the aim to measure the systematic error of the η-algorithm. The analysis of the collected data [6] clearly confirms the presence of an angle-dependent shift, and the correction proposed in ref. [3] is able to cancel the shift at any measured angle.

In this work we concentrate the attention on an anomaly observed on the data of ref. [6] where the average of the COG distribution is appreciably different from zero for orthogonal particle incidence. In the absence of magnetic field, the maximal symmetry is expected for this configuration with the COG probability distribution symmetric respect to the origin and zero average. The non zero average could be originated by an asymmetry in the charge drift to the collection pads or some other (linear) distortion in the read-out chain.

Our correction to the η-algorithm works identically for asymmetrical response functions, but, a further detector parameter must be known: the COG position of the strip response function. In fact, the COG algorithm assumes that the strip signals are concentrated in the COG position of the strip response function. The asymmetry moves the COG response function from the strip axis, and this shift must be accounted for in any reconstruction at any angle, not only in the η-algorithm.

We have no control on the physics of the showering particle, but, we suppose to know all the

detector parameters, being the detector production under our control. In practice the situation is not so simple. Various types of material depositions are performed in specialized places and slight asymmetries could be easily introduced during these operations, no visual or electronic inspection can isolate these defects. In addition to this, subtle asymmetries could be introduced in the path of the data from the detector to final user.

Direct measurements could be performed, but they require auxiliary detectors with resolutions much better than the tested detectors. It is evident the complexity of this task. We will tray to estimate the asymmetry from the charge collected by the strips for MIP at orthogonal incidence angle. In this way, a good angular measurement can replace a high resolution position measurements.

In section 2 we give a direct demonstration of the η-algorithm correction in general cases to isolate the effects of the asymmetry. Section 3 is devoted to define our strategy to estimate the asymmetry parameter of the response functions and to test it on simulated data with two different type of asymmetry. Our simulations are tuned on the double sided silicon microstrip detectors of the type introduced by ref. [7, 8], and used in the PAMELA detector. In one side a strip each two is left unconnected, and it distributes the charge in a peculiar mode. We call this side floating strip side. The other side is normal (in the sense that it has no floating strips).

Section 4 deals with the non orthogonal particle incidence and its relation with the asymmetry. The angular rotation introduces a simple and almost linear effect that allows a better determination of the asymmetry. It gives even an indication of the angular precision to obtain significative results. This sensitivity to the angular rotation suggests a method to measure the Lorentz angle when a magnetic field is present. Here, the effect of a magnetic field an a silicon microstrip detector is simulated as an effective rotation of the incoming particle direction. A proper angular rotation is able to restore the maximal symmetry to the signal distribution. Our method easily find this condition even in presence of an asymmetry of the response function. The simulations of this case show an excellent sensitivity of the method.

We are aware that these developments are very formal and complex, but the asymmetry correction and the Lorentz angle are deeply buried in the properties of the COG algorithm. It is interesting that analytical developments are able to isolate them and reach the consistency displayed by the simulations.

2. Correction of the systematic errors

2.1 COG averages

In ref. [1, 2, 3] we extensively utilized the Fourier Transform (FT) and Poisson identity [9, 10] (or the Shannon sampling theorem). Now, we will proceed in a different way that avoids some technical complications and underlines its generality.

Let us derive the COG average. With the notation of [1, 2] and considering all the strips with a non zero energy, we have the following definition for the COG (τ is the strip dimension):

$$x_g(\varepsilon) = \frac{\sum_{n\in\mathbb{Z}} n\tau\ \mathrm{f}(n\tau-\varepsilon)}{\sum_{n\in\mathbb{Z}} \mathrm{f}(n\tau-\varepsilon)} \tag{2.1}$$

where $\mathrm{f}(n\tau-\varepsilon)$ is the energy collected by a strip centered in $n\tau$ for a signal distribution with its COG in ε (for any $\varepsilon\in\mathbb{R}$). We use an infinite sum, but the function $\mathrm{f}(n\tau-\varepsilon)$ is expected to go

to zero for a fixed range of its argument (finite support function). An identical transformation on equation 2.1 gives:

$$x_g(\varepsilon) - \varepsilon = \frac{\sum_{n\in\mathbb{Z}}(n\tau-\varepsilon)\mathrm{f}(n\tau-\varepsilon)}{\sum_{n\in\mathbb{Z}}\mathrm{f}(n\tau-\varepsilon)}\,. \tag{2.2}$$

Equation 2.2 explicitly shows the τ-periodicity of $x_g(\varepsilon)-\varepsilon$ and justifies the use of Fourier Series (FS). The assumption of absence of signal loss gives a flat efficiency surface and $\mathrm{f}(n\tau-\varepsilon)$ has the sum rule:

$$\sum_{n\in\mathbb{Z}} \mathrm{f}(n\tau-\varepsilon) = 1 \quad \forall\varepsilon\in\mathbb{R}, \tag{2.3}$$

allowing the suppression of the denominator in equation 2.2. The energy $\mathrm{f}(n\tau-\varepsilon)$ is defined as the convolution of the strip response function $\mathrm{g}(x)$ with the signal distribution $\varphi(x-\varepsilon)$. The response function $\mathrm{g}(x)$ is centered on the fiducial strip position and $\varphi(x)$ has its COG in ε:

$$\mathrm{f}(n\tau-\varepsilon) = \int_{-\infty}^{+\infty} \mathrm{g}(n\tau-x')\varphi(x'-\varepsilon)\mathrm{d}x' \tag{2.4}$$

With equation 2.3, the ε-average on a period τ of equation 2.2 acquires an easy aspect. The introduction of the integration variables $\xi_n = n\tau-\varepsilon$ gives:

$$\frac{1}{\tau}\int_{-\tau/2}^{+\tau/2}(x_g(\varepsilon)-\varepsilon)\mathrm{d}\varepsilon = \frac{1}{\tau}\sum_{n\in\mathbb{Z}}\int_{n\tau-\tau/2}^{n\tau+\tau/2}\xi_n\,\mathrm{f}(\xi_n)\mathrm{d}\xi_n\,,$$

the sum on n can be absorbed in the definition of the integration limits:

$$\frac{1}{\tau}\int_{-\tau/2}^{+\tau/2}(x_g(\varepsilon)-\varepsilon)\mathrm{d}\varepsilon = \frac{1}{\tau}\int_{-\infty}^{+\infty}\xi\;\mathrm{f}(\xi)\mathrm{d}\xi \tag{2.5}$$

Equation 2.5 is the first momentum of $\mathrm{f}(x)$, and the convolution theorem for the first momenta [9] gives:

$$\int_{-\infty}^{+\infty}\xi\;\mathrm{f}(\xi)\mathrm{d}\xi = \delta_g\tau+\delta_\varphi$$

Where δ_g and δ_φ are defined as:

$$\delta_g = \frac{1}{\tau}\int_{-\infty}^{+\infty}\xi\,\mathrm{g}(\xi)\,\mathrm{d}\xi \qquad \delta_\varphi = \int_{-\infty}^{+\infty}\xi\,\varphi(\xi)\,\mathrm{d}\xi$$

For their normalizations ($\int_{-\infty}^{+\infty}\varphi(\xi)\mathrm{d}\xi = 1$ and $\int_{-\infty}^{+\infty}\mathrm{g}(\xi)\mathrm{d}\xi = \tau$), δ_g is the COG position of the response function and δ_φ is the COG position of the signal distribution. The COG δ_φ is zero for our definition of ε, and the average of equation 2.2 remains:

$$\frac{1}{\tau}\int_{-\tau/2}^{+\tau/2}(x_g(\varepsilon)-\varepsilon)\mathrm{d}\varepsilon = \delta_g\,. \tag{2.6}$$

Equation 2.6 shows that the COG algorithm is a biased estimator of the impact point. To eliminate this bias, equation 2.6 imposes that the fiducial strip position must be coincident with the COG of its response function $\mathrm{g}(x)$, in this case $\delta_g = 0$. Any deviation from this condition introduces a constant shift in the reconstructed position.

In principle, the extraction of δ_g from the data is easy, one has to take a set of (uniform) events, where the values of $\{\varepsilon_j\}$ are known, and to average the differences $x_g(\varepsilon_j) - \varepsilon_j$. In practice, the value of ε_j is very difficult (or impossible) to measure with the due precision. Thus, we have to find another strategy to obtain a reasonable estimation of δ_g from the data of a standard test beam experiment.

Equation 2.6 is evidently valid for a noiseless case. The data are surely noisy. Assuming a symmetric additive noise, it is easy to figure out how it will modify the COG. At fixed impact point the noise will spread the data around the noiseless COG value. The symmetry of the noise distribution induces a symmetric distribution of COG values around the noiseless one and the averages of the noisy data will converge to the noiseless ones. So, for a large data sample, our noiseless equations will work identically even in presence of noise.

2.2 The η-Algorithms

Let us see how δ_g modifies the correction of the η algorithms. As we proved in refs. [1, 3], η-algorithms may be extended beyond the two strip case used in ref. [4], and identified as a general property of any COG algorithms. Due to their strict similarity, we will continue to call η-algorithms all these extensions.

The COG algorithms with different numbers of signal strips have very different properties and systematic errors, and a great care must be devoted to avoid to mix them. For example, the cuts on small or negative values of signal strips may produce the mixing. In ref. [3], 2-strips, 3-strips and 4-strips algorithms exhausted our needs, there we limited to consider incidence angles up to 20°. Above 20°, 5 or more strips are relevant, and other strategies can be used to reduce these cases to the present developments.

In the simulations, the set of events has ε-values with a uniform distribution on a strip. This assumption supports our averages over ε. As in ref. [3] we calculate the COG in a reference system bound to the event, we choose the maximum signal strip. The experimental events are spread over a large number of strips. To be consistent with our simulations, we will assume that the set of events $\{\varepsilon(j)\}$ produces the uniform distribution of points $\{\sum_{K\in\mathbb{Z}} \varepsilon(j) + K\tau\}$. Thus, on a given strip, one has the uniform distribution of points $\{\varepsilon(j) + K_j\tau\}$, where $K_j\tau$ is the distance of the strip with the impact point $\varepsilon(j)$ from the given strip. This will be the definition of uniformity of events on a strip.

Let us recall some aspects of the η algorithm [3] to define the notation. Assuming the existence of a single valued function $x_{gk}(\varepsilon)$ which is randomly sampled by our COG algorithm with $k-$strips (in the following the index k will indicate the number of strips used in the algorithm), the probability to have x_{gk} is:

$$P(\varepsilon)\left|\frac{\mathrm{d}\varepsilon}{\mathrm{d}x_{gk}}\right| = \Gamma(x_{gk})\,,$$

where $P(\varepsilon)$ is the probability to have a value ε and $\Gamma(x_{gk})$ is the corresponding probability for x_{gk}. The positivity of the derivative is reported in ref. [1] and it turns out that any incoming signal, with average positive signal distribution, has positive derivative. Assuming a constant probability $P(\varepsilon) = 1/\tau$, one arrives to the first order differential equation:

$$\frac{1}{\tau}\frac{\mathrm{d}\varepsilon}{\mathrm{d}x_{gk}} = \Gamma(x_{gk})\,. \tag{2.7}$$

The integration of equation 2.7 requires an initial constant (i.e., an exact value of the impact point $\varepsilon(x_{gk})$). For symmetric signal distribution and symmetric response function, the initial constant is the center of the strip or one of its border. These special points have $x_{gk} = \varepsilon$. For the asymmetric case, the initial constant must be determined resorting to other properties of the COG algorithms.

The presence of noise modifies this picture introducing an average over the noise realization. To render the approach less heavy we will neglect this average, but now equation 2.7 becomes the definition of the function $\varepsilon_k(x_{gk})$.

The uniform distribution of events ε_j on the array of periodic detector generates a periodic probability distribution $\Gamma^p(x_{gk})$ (normalized on a period), and the solution of equation 2.7, for the symmetric configuration, is given by:

$$\varepsilon_k(x_{gk}) = -\frac{\tau}{2} + \tau \int_{-\tau/2}^{x_{gk}} \Gamma^p(x)\mathrm{d}x \tag{2.8}$$

The initial constant used in [4] is $\varepsilon_k(x_{gk} = 0) = 0$, but, as we discussed above, $\varepsilon_k(x_{gk} = -\tau/2) = -\tau/2$ and $\varepsilon_k(x_{gk} = 0) = 0$ are exact for symmetric $\varphi(x)$ and for symmetric response function. In all the other cases, the required correction will be indicated with Δ_{0k}.

It is easy to show the periodicity of $\varepsilon_k(x_{gk}) - x_{gk}$, in fact, due to the periodicity and the normalization of Γ^p we may rewrite the equation 2.8 as:

$$\varepsilon_k(x_{gk}) = x_{gk} + \int_{-\tau/2}^{x_{gk}} (\tau\Gamma^p(x) - 1)\mathrm{d}x\,. \tag{2.9}$$

The integral is a periodic function of x_{gk}, and we express it as a FS:

$$\begin{aligned} \varepsilon_k(x_{gk}) &= x_{gk} + \sum_{n=-\infty}^{+\infty} \alpha_n \mathrm{e}^{(\mathrm{i}2\pi n x_{gk}/\tau)} \\ \alpha_n &= \frac{1}{\tau}\int_{-\tau/2}^{+\tau/2} [\varepsilon_k(x_{gk}) - x_{gk}]\,\mathrm{e}^{(-\mathrm{i}2\pi n x_{gk}/\tau)}\mathrm{d}x_{gk}, \end{aligned} \tag{2.10}$$

and with the correction Δ_{0k}:

$$\varepsilon_k(x_{gk}) = x_{gk} + \sum_{n=-\infty}^{+\infty} \alpha_n \exp(\mathrm{i}2\pi n x_{gk}/\tau) + \Delta_{0k}\,. \tag{2.11}$$

In the definition of the α_n, the k-index, the number of strips used in the algorithm, is not explicitly reported, but it is evident that α_n depends from k.

With low noise, the function $\varepsilon_k(x_{gk})$ is a good approximation of noiseless form, and it sits on the most probable values of ε for any x_{gk}. This property is crucial for any best fit in a track reconstruction. The absence of the correction Δ_{0k} introduces an average systematic shift of ε_k respect to the true ε, quite evident in the simulations.

2.3 Correction of the η Algorithms

We calculate Δ_{0k} exploring the mean value of the differences $\varepsilon_k(j) - \varepsilon(j)$ in a case of a large number N of events and uniform distribution on a given strip as defined. The mean value must be

zero in the absence of systematic errors:

$$\frac{1}{N}\sum_{j=1}^{N}[\varepsilon_k(j)-\varepsilon(j)] = \frac{1}{N}\sum_{j=1}^{N}[x_{gk}(j)-\varepsilon(j)] + \frac{1}{N}\sum_{j=1}^{N}[\sum_{n=-\infty}^{+\infty}\alpha_n\, e^{(i2\pi n x_{gk}(j)/\tau)}] + \Delta_{0k} \tag{2.12}$$

The mean value of the FS, weighted with the probability $\Gamma^p(x_{gk})$, gives α_0 [3]. Adding and subtracting the position of the strip with the maximum signal μ_j, equation 2.12 becomes:

$$\frac{1}{N}\sum_{j=1}^{N}[\varepsilon_k(j)-\varepsilon(j)] = \frac{1}{N}\sum_{j=1}^{N}[x_{gk}(j)-\mu_j] - \frac{1}{N}\sum_{j=1}^{N}[\varepsilon(j)-\mu_j] + \alpha_0 + \Delta_{0k} \tag{2.13}$$

The mean of $(\varepsilon(j)-\mu_j)$ is independent from the COG algorithm, and we calculate it in the easier condition. We use equation 2.6 with all the signal strips in the COG algorithm (four or five at most), to near the condition of equation 2.3. We will call this $x_{g\infty}$, and equation 2.6 becomes:

$$\frac{1}{N}\sum_{j=1}^{N}(x_{g\infty}(j)-\mu_j) = \frac{1}{N}\sum_{j=1}^{N}(\varepsilon(j)-\mu_j) + \delta_g\,. \tag{2.14}$$

The average of $\varepsilon(j)-\mu_j$ of the unknown exact impact points is reduced to known quantities. Substituting in equation 2.13, and imposing the zero average of $(\varepsilon_k(j)-\varepsilon(j))$ the equation for Δ_{0k} becomes:

$$\frac{1}{N}\sum_{j=1}^{N}(x_{gk}(j)-\mu_j) - \frac{1}{N}\sum_{j=1}^{N}(x_{g\infty}(j)-\mu_j) + \delta_g + \alpha_0 + \Delta_{0k} = 0$$

$$\Delta_{0k} = \frac{1}{N}\sum_{j=1}^{N}(x_{g\infty}(j)-\mu_j) - \frac{1}{N}\sum_{j=1}^{N}(x_{gk}(j)-\mu_j) - \alpha_0 - \delta_g$$

We have to recall that the two expressions $\sum_{j=1}^{N}(x_{g\infty}(j)-\mu_j)/N$ and $\sum_{j=1}^{N}(x_{gk}(j)-\mu_j)/N$ are the averages of the COGs calculated in our reference system of the maximum signal strip. The constant α_0 embodies the initial conditions (not limited to 0 or $-\tau/2$) and the correction Δ_{0k} eliminates any reference to the initial integration contant.

To be complete, the correction $\Delta_{0k}+\alpha_0$ eliminates even the systematic error of the COG algorithm (with k-strips) due to the non zero δ_g and to the eventual loss given by the limitation in the strip number. The loss has rarely a significative effect, but we are able to consider it. For the COG indicated with $x_{g\infty}$ the correction is simply $-\delta_g$. The residual non zero average is the mean value of $(\varepsilon(j)-\mu_j)$ that the asymmetry modifies respect to its zero value in the symmetric case.

In the simulations of ref. [3], the COG algorithm with four strips was a good approximation for $x_{g\infty}$, here we will use even the five strip algorithms. Due the physical meaning of δ_g, once its value is obtained, the correction of any position algorithm and for any incidence angle can be implemented. In the following we will need the correction $\Delta_{0\infty}$ to the η-algorithm obtained starting from $x_{g\infty}$, this correction is given by $-\alpha_0-\delta_g$.

An indication of $\delta_g \neq 0$ is given by a non zero value of the average of $(x_{g\infty}(j)-\mu_j)$ for the orthogonal incidence. This averages can not be zero for equation 2.14. It is a sum of two unknown quantities, and another equation is necessary to extract their values. To estimate δ_g, we need to reconstruct $\varphi(\varepsilon)$ and explore its asymmetry.

3. Determination of δ_g

3.1 Signal reconstruction

In refs. [1, 3] we demonstrated an equation to obtain the signal distribution from the COG algorithm. The $\varphi(\varepsilon)$ is given by:

$$\frac{\mathrm{d}x_g(\varepsilon)}{\mathrm{d}\varepsilon} = \tau \sum_{n\in\mathbb{Z}} \varphi(n\tau - \varepsilon - \tau/2)\,. \tag{3.1}$$

In the derivation of equation 3.1 the response function is assumed to be the lossless interval function, and $\varphi(x)$ is the signal distribution. The expression 3.1 is the sum of copies of $\varphi(\tau/2-\varepsilon)$ shifted of $n\tau$ with $n \in \mathbb{Z}$. This gives a periodic function with overlaps of the tails (aliasing) if the range of $\varphi(x)$ is greater than τ. For ranges less than τ the reconstruction is faithful. If the range of $\varphi(x)$ is greater than τ, the assembly of a set of contiguous interval functions avoids this limitation.

For fluctuating signal distributions, as in the case of a MIP, equation 3.1 defines an average signal distribution.

3.2 Generic Response Function

The reconstruction of $\varphi(x)$ of equation 3.1 requires the response function as a pure interval function of size τ, rarely this condition is verified, and a generic response function produces a redefinition of $\varphi(x)$. If the lossless condition equation 2.3 is maintained, we proved in ref. [1] that the response function must be a convolution of an interval function with another (arbitrary and eventually asymmetric) function $\mathrm{g}_1(x)$. In this case, the function of Eq. 3.1 is the convolution of the true signal distribution with $\mathrm{g}_1(x)$. We will continue to call $\varphi(x)$ any result of $\mathrm{d}x_g(\varepsilon)/\mathrm{d}\varepsilon$ even if it deviates from the true signal distribution.

In ref. [3], we explored a possible form of the response function for microstrip detector with floating strips, and the following form reproduces the main aspects of the data:

$$\begin{aligned} p(x) = \int_{-\infty}^{+\infty} \Pi(x-x')\big\{0.45\,[\delta(x'-1/4) + \delta(x'+1/4)] \\ + 0.05[\,\delta(x'-1/2) + \delta(x'+1/2)]\big\}\,. \end{aligned} \tag{3.2}$$

(This form is surprisingly similar to that measured in ref. [11].) Here, the reconstruction of equation 3.1 generates the convolution of the signal distribution with the four Dirac δ-functions of equation 3.2, the low intensity Dirac δ-functions have a negligible effect, but the effects of the two main δ's are clearly seen in figure 1 as two copies of the signal distribution.

If the response function is asymmetric, the asymmetry is contained in $x_g(\varepsilon)$ and transferred to the reconstructed function. The asymmetry transfer to $\varphi(x)$ does not allow a direct extraction of δ_g. We have to resort to an indirect procedure.

3.3 Inverse function of $\varepsilon_k(x_{gk})$

The form of equation 2.10 for $\varepsilon_k(x_{gk})$ is not well suited for our needs. Its inverse function $x_{gk}(\varepsilon_k)$ is of better use, and it is expressed by:

$$x_{gk}(\varepsilon_k) = \varepsilon_k + \sum_{n=-L}^{+L} \beta_n \exp(\mathrm{i}\frac{2\pi n}{\tau}\varepsilon_k) \tag{3.3}$$

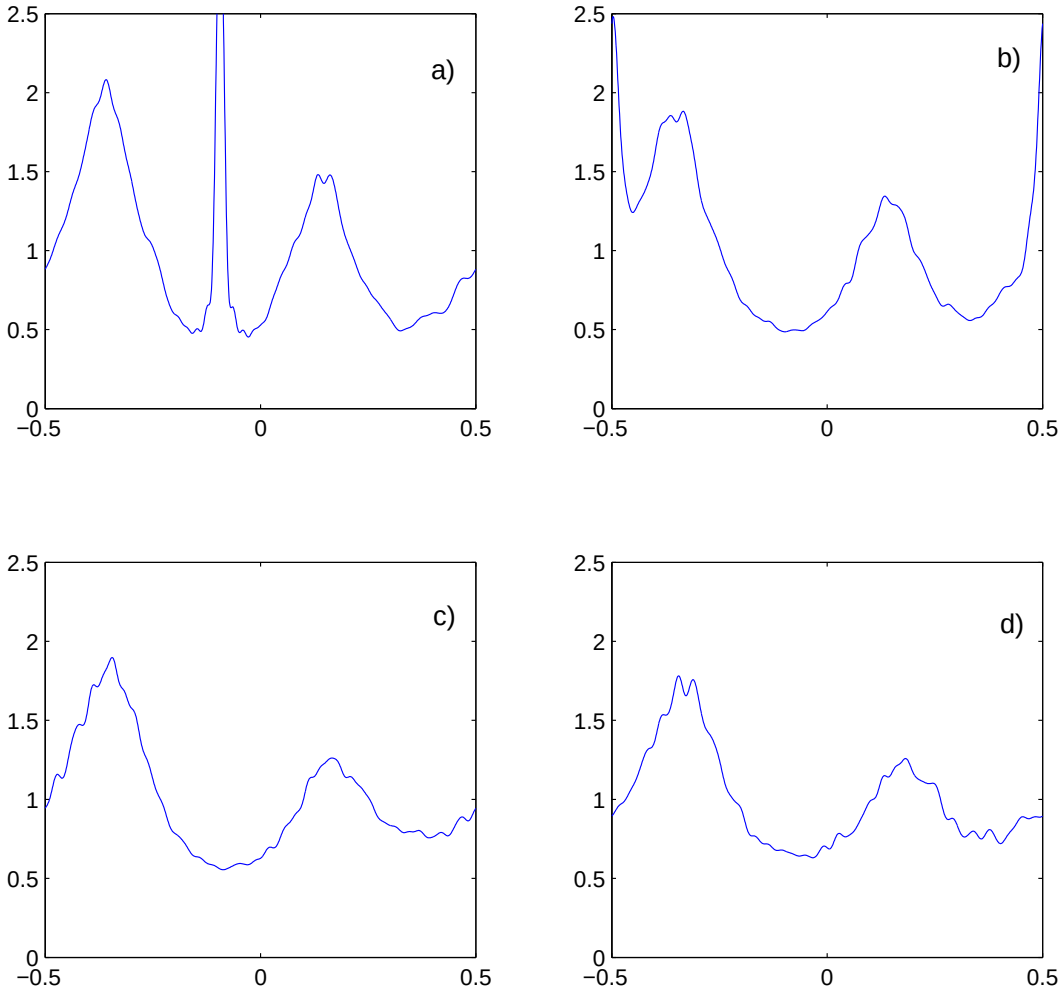

Figure 1. *Reconstruction of $\varphi(x_k)$ (with noise) using different numbers of strips: a) with 2 strips, b) with 3 strips, c) with 4 strips, d) with 5 strips. The asymmetry parameter is 0.07 and 45000 events.*

$$\beta_n = \frac{1}{\tau}\int_{-\tau/2}^{\tau/2}\left[x_{gk} - \varepsilon_k(x_{gk})\right]\exp\left(-\mathrm{i}\frac{2\pi n}{\tau}\varepsilon_k(x_{gk})\right)\Gamma^p(x_{gk})\mathrm{d}x_{gk}$$

where $\varepsilon_k(x_{gk})$ is the result of equation 2.8 and L the maximum wave-number used, L around 45 is a reasonable cut off even if the limits $\pm\infty$ will be often used. All the forms of $\varphi(x)$ are obtained differentiating equation 3.3 respect to ε_k.

As discussed, deformations are introduced in $\varphi(x)$ by the differences of $p(x)$ respect to an interval function. Another set of important deformations are produced by the loss. Two type of loss are encountered: the intrinsic loss of the strip and the loss given by the suppression of non-zero signal strips. The first type of loss operates as an additional smooth deviation of the response function from the pure interval function, it has a negligible effect on our procedures. The second type of loss introduces a strong deformations in $\varphi(x)$. The presence of any type of loss is explicitly excluded by the form of equation 3.1, but we can, in any case, differentiate equation 3.3 and explore its results. In the absence of noise, the deformations given by the second type of loss assume the

form of Dirac δ-functions. The limitation in the number of terms in equation 3.3 gives finite peaks. The exclusion of signal strips in the COG algorithm generates forbidden x_g-values. Here the probability Γ^p is zero and $\varepsilon(x_g)$ has an interval of constant value. If we insist to invert the function $\varepsilon(x_g)$ this constant horizontal segment becomes a vertical segment, and the differentiation generates a Dirac δ-function. In general, if the strip number is even, one aspects peaks around $\varepsilon_k \approx 0$, for odd strip numbers the peaks are for $\varepsilon_k \approx \pm\tau/2$. The amplitudes of the peaks are proportional to amplitude of the signal function acquired by the excluded strips [1]. For $k = 2,3$ clear peaks are present in the reconstructions of ref. [3] and figure 1. For $\delta_g \neq 0$ and $k = 2$, the peak is not in zero due to the $-1/2$ as the lower integration limit of equation 2.8, this fixes $\varepsilon_k = -1/2$ to coincide with $x_{gk} = -1/2$. In fact, the peaks of x_{g3} are at $\varepsilon_3 = \pm 1/2$. With the lower integration limit to zero, $\varepsilon_k = 0$ coincides with $x_{gk} = 0$ and the peak for $k = 2$ would be at $\varepsilon_2 = 0$. It is evident that with an asymmetry in the response function nor $x_{gk} = -1/2$ nor $x_{gk} = 0$ are exact, and Δ_{0k} fixes the correct ε_k and the correct positions of the peaks. The almost total suppression of the loss eliminates the peaks for $k = 4$ and $k = 5$ in figure 1.

A due care must be devoted to avoid numerical instabilities. Intervals where equation 3.3 does not exist (due to zero values of Γ^p) are easily encountered in noiseless case. The noise helps to avoid $\Gamma^p = 0$, but it easily adds other unwanted artifacts. The Cesaro's method of arithmetic means [10] attenuates some numerical instabilities.

3.4 Analytical form of $x_g(\varepsilon)$

The exploration of the analytical form of $x_g(\varepsilon)$ clarifies our path toward δ_g. Here all the properties of the detector and the signal distribution are explicitly underlined. In the case of orthogonal incidence, the incoming signal distribution is symmetric and its FT $\Phi(\omega)$ is real and symmetric. The response function $\mathrm{p}(x)$ has asymmetries and its FT $P(\omega)$ is complex with $P(-\omega) = P^*(\omega)$. The form of $x_g(\varepsilon)$, with δ_g the first momentum of $p(x)$, is [3] (with $\tau = 1$):

$$x_g(\varepsilon) = \varepsilon + \delta_g + i \sum_{k\neq 0, k=-\infty}^{+\infty} \Phi(-2k\pi)\mathrm{P}'(-2k\pi)\exp(i2k\pi\varepsilon)\,, \tag{3.4}$$

where $\mathrm{P}'(\omega)$ is the first derivative of $\mathrm{P}(\omega)$ respect to ω, and ε is the impact point. We know that, even in the best condition, the equation 2.8 for ε_k has an incorrect initial constant. To handle the asymmetric case, we have to generalized a new $\overline{\varepsilon}_k(x_{gk})$ defined for any initial condition x^0_{gk} beyond the $x^0_{gk} = -1/2$ of equation 2.8:

$$\overline{\varepsilon}_k(x_{gk}) = x^0_{gk} + \int_{x^0_{gk}}^{x_{gk}} \Gamma(x)^p \mathrm{d}x$$

The correction procedure must work for any x^0_{gk}. It is evident that $x^0_{gk} = -1/2$ or $x^0_{gk} = 0$ have the minimal corrections being exact in the symmetric case. The constant $\varepsilon(x^0_{gk}) - x^0_{gk}$ is now the difference of $\overline{\varepsilon}_k$ from ε, given the initial constant x^0_{gk}. Substituting ε with $\overline{\varepsilon}_k$ in equation 3.4, we have:

$$\varepsilon = \overline{\varepsilon}_k + (\varepsilon(x^0_{gk}) - x^0_{gk})$$

$$x_g(\overline{\varepsilon}_k) = \overline{\varepsilon}_k + (\varepsilon(x^0_{gk}) - x^0_{gk}) + \delta_g + \sum_{n\neq 0, n=-\infty}^{+\infty} \widetilde{\beta}_n \exp[i2n\pi(\overline{\varepsilon}_k + \varepsilon(x^0_{gk}) - x^0_{gk})]\,. \tag{3.5}$$

Remembering equation 3.3, the comparison with equation 3.4 gives:

$$\begin{aligned}
\beta_n &= \widetilde{\beta}_n \exp[i\,2n\pi(\varepsilon(x^0_{gk}) - x^0_{gk})] \quad n \neq 0 \\
\beta_0 &= (\varepsilon(x^0_{gk}) - x^0_{gk}) + \delta_g \\
\widetilde{\beta}_n &= i\,\Phi(-2n\pi)\mathrm{P}'(-2n\pi)
\end{aligned} \tag{3.6}$$

as expected β_0 is the sum of the two unknown δ_g and the shift $(\varepsilon(x^0_{gk}) - x^0_{gk})$. To extract δ_g we need another equation. The derivative $\mathrm{d}x_g(\overline{\varepsilon}_k)/\mathrm{d}\overline{\varepsilon}_k$ does not contain β_0, it has a shift of $(\varepsilon(x^0_{gk}) - x^0_{gk})$ respect to the differentiation in the exact ε. This shift is present as a phase factor in equation 3.6, and it goes to increase the asymmetry of $\varphi(\overline{\varepsilon}_k)$. In the symmetric configuration the phase relations are easy: all the $\Phi(-2n\pi)\mathrm{P}'(-2n\pi)$ are real and $\widetilde{\beta}_n$ imaginary.

Due to the special form of the of the relation of β_n and $\widetilde{\beta}_n$, we can add a fictitious phase parameter $2\pi n\xi$ to β_n to modify the asymmetry of $\varphi(\overline{\varepsilon}_k)$. For small asymmetry, we expect that this asymmetry variation of $\varphi(\overline{\varepsilon}_k)$ reaches its minimum when all the β_n coincide with $\widetilde{\beta}_n$. The phase factors of the $\widetilde{\beta}_n$ are given by the intrinsic asymmetry of the response function, and are non trivial functions of n. These phase relations are not eliminated by the trivial transform implied by a global shift of φ and the intrinsic asymmetry cannot be reduced. An asymmetry parameter with a small sensitivity to the noise is:

$$\Omega(\xi) = \int_{-1/2}^{1/2} \left[\varphi(\xi + \overline{\varepsilon}_k) - \varphi(\xi - \overline{\varepsilon}_k)\right]^2 \mathrm{d}\overline{\varepsilon}_k\,. \tag{3.7}$$

Here $\varphi(\overline{\varepsilon}_k)$ is $\mathrm{d}x_g(\overline{\varepsilon}_k)/\mathrm{d}\overline{\varepsilon}_k$. The minimum of $\Omega(\xi)$ is obtained for a ξ_m given by:

$$\xi_m = -(\varepsilon(x^0_{gk}) - x^0_{gk})\,,$$

this is the second equation that allows the use of β_0 in equation 3.6 to extract δ_g:

$$\delta_g = \beta_0 + \xi_m\,. \tag{3.8}$$

$\Omega(\xi)$ is expressed with β_n as:

$$\Omega(\xi) = 2\sum_{n\in\mathbb{Z}} \left[|\beta_n|^2 + \beta_n^2 \exp(\mathrm{i}4\pi n\xi)\right](2\pi n)^2\,. \tag{3.9}$$

The first term is a constant and the ξ-dependence is a periodic function of period $1/2$. When $\delta_g = 0$ and $x^0_{gk} = 0$ or $-1/2$ and $\beta_n = \widetilde{\beta}_n$ it is easy to verify the minimum for $\xi = 0$ given that $\widetilde{\beta}_n^{\,2} = -|\beta_n|^2$. In general, the minima of equation 3.9 produce the corrections of the η-algorithm for all the initial x^0_{gk}.

To see the effectiveness of the minimization of equation 3.9, we calculated $\Omega(\xi)$ with $\xi = 0$ for all the initial conditions x^0_{gk} from -1 and 0. In this case $\Omega(0)$ has minima where $\beta_n = \widetilde{\beta}_n$ or, more precisely, in the points where $\varepsilon^0_k - x^0_{gk} = 0$. In figure 2 we report $\Omega(0)$ in function of the initial x^0_{gk} and effectively it has evident minima when $\varepsilon^0_k - x^0_{gk} = 0$. In the simulations we use a low asymmetry $\zeta = 0.02$, and a noiseless simulation and x_{g4} algorithm for a floating strip sensor. Figure 2 gives an empirical support to our research of the minima for $\Omega(\xi)$.

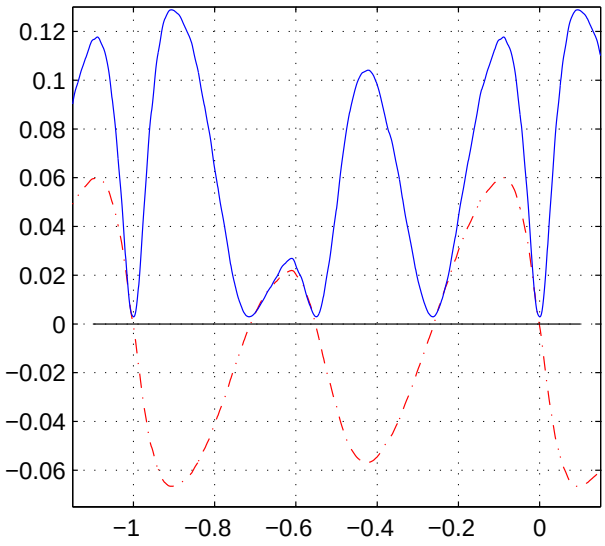

Figure 2. *Continuous line (blue): Asymmetry $\Omega(0)$ calculated for all the initial conditions x^0_{g4} from -1 to 0. The dash-dotted line (red) is the correction $\varepsilon^0_4 - x^0_{g4}$, the asymmetry has minima when $\varepsilon^0_4 - x^0_{g4} = 0$. Noiseless simulation with $\zeta = 0.02$ and floating strip sensor*

In general, any initial condition can be used, but, the ξ_m are widely different with an inefficient minimum search. The special form of (β_0) and the following substitution simplifies the search and eliminates the explicit dependence from the initial conditions:

$$\begin{aligned} \beta'_n &= \beta_n \exp(-\mathrm{i}\, 2\pi n \beta_0) \\ \beta'_n &= \widetilde{\beta}_n \exp(-\mathrm{i}\, 2\pi n \delta_g)\,, \end{aligned} \tag{3.10}$$

and, for any x^0_{gk}, equation 3.8 is reduced to:

$$\delta_g = \xi_m\,.$$

A presence of a small loss has a negligible effect on this approach. Large loss, signaled by the presence of peaks around zero or $\pm 1/2$, can strongly modify the minimum search.For example, in our first set of simulations, x_{g2} and x_{g3} have minima very different from that of x_{g4}, x_{g5}.

3.5 Simulations

The simulated data are generated as discussed in ref. [3]. For the floating strip case, we modify the response function breaking the symmetry of the two most important Dirac-δ functions of equation 3.2. We add to the first Dirac-δ function a constant ζ and a ζ is subtracted to the other one to save the normalization, figure 1 has $\zeta = 0.07$. This type of asymmetry looks similar to the one observed in the test-beam data, but we amplify the effect. In any case, this is only a numerical experiment to see the efficiency of the δ_g determination. We will compare with the noiseless simulation to see the effect of the noise.

Figure 3 shows the determination of δ_g with the procedure illustrated above. The simulated data are noiseless, but even here we see fluctuations of δ_g from equation 2.14. The fluctuations

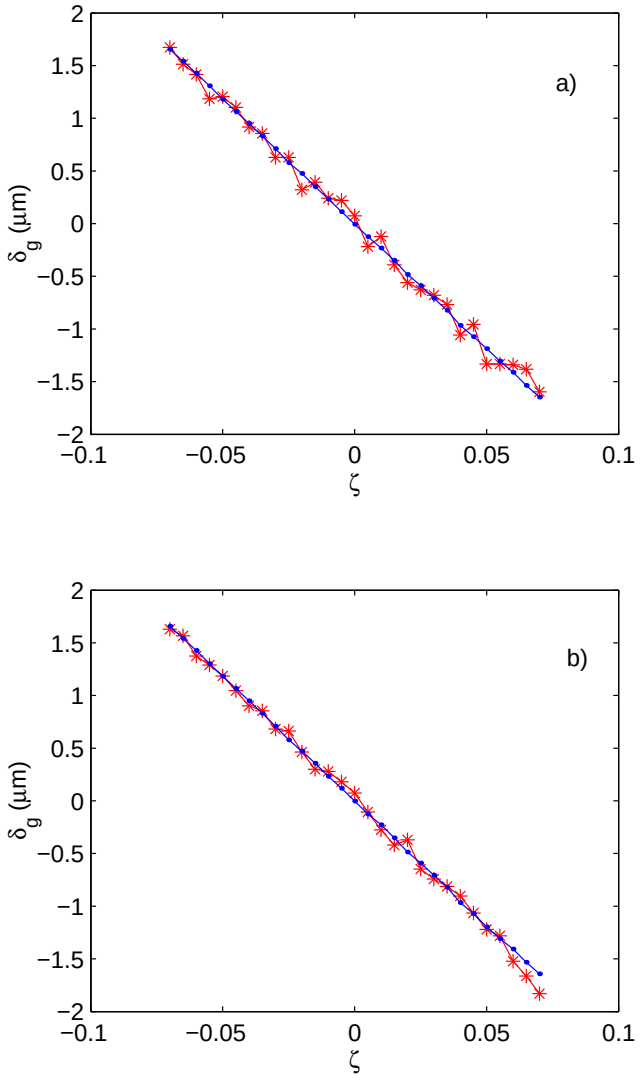

Figure 3. *Noiseless case, the blue dots are the results of equation 2.14, the red asterisks are the δ_g obtained by the minima of equation 3.9. The plot a is given by x_g with four strips and b with five strips.*

originate from the reconstruction that requires the extraction of $\varphi(\varepsilon)$ from histograms and, due to a finite set of data (45000 events), the procedure adds an effective noise that is lower in the case of δ_g calculated with five strips. Here the attenuation of the fluctuations could be due a reduction of the slight loss, that is present in the four strip simulation due to the suppression of the signal (convolution of gaussians [3]) collected by the fifth strip. This loss is too low to produce a peak, but it contributes to the effective noise of Γ^p.

The realistic case (with noise) fluctuates more than the noiseless case. Even here the δ_g calculated with five strips has less fluctuations than that calculated with four strips. The RMS error is 0.1 μm for the five strips case and 0.2 μm for the four strips case. In figure 4 we reported the averages $\sum_{j=1}^{N}(x_{gk}(j)-\mu_j)/N$ that is the signal of a non zero δ_g. The form of asymmetry generation, we used, gives an amplification of the COG averages by (relatively) small δ_g. For the floating strip

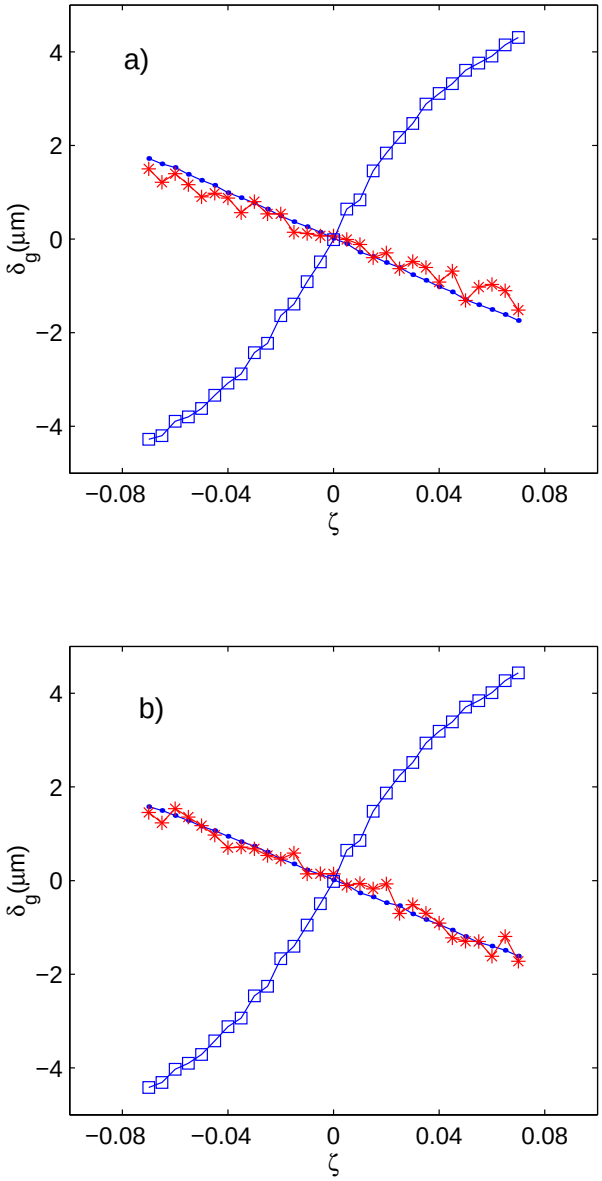

Figure 4. *Noisy case. The dots are the results of equation 2.14.The asterisks are the δ_g given by the minima of equation 3.9,and the squares are the COG averages. Plot a) is for the four strip x_g and b) is for the five strip x_g.*

side, the introduction of δ_g could be a minor correction around half micron, with all the sensors oriented identically a parallel shift of the track is implied. If some sensor has a reverse orientation δ_g change sign and gaps of a micron are present in the tracks. Even if these constant shifts could be corrected by the alignment procedures, it is a good practice to have estimators free of bias when possible.

3.6 Normal strips

We explore the strategy of the extraction of δ_g for the case of "normal" strips. Even now the impact direction is orthogonal to the detector plane. At this angle, the detector resolution is low due to the concentration of a large parte of the signal in a single strip. To be consistent with the real detector, the simulated noise is doubled respect to the case of the floating strip sensor, and its effect strongly deteriorates the extraction of δ_g. Here we have no indications of the type of asymmetry, the mean value of x_{g4} is different from zero, but the reconstruction does not show evident asymmetry. We produce the asymmetry with an additional Dirac-δ function $\zeta\,\delta(x-\tau/4)$ convoluted with the usual interval function to have an everywhere flat efficiency. The values of ζ are all positive, we must avoid negative values of the response function and of $\mathrm{d}x_g(\varepsilon)/\mathrm{d}\varepsilon$.

For the noiseless case, the reproduction of δ_g is reasonable for all the ζ values even if the fluctuations introduced by the finite number of events is higher than the corresponding case of the floating strips. The addition of the noise changes drastically the results, the determination of δ_g degrades rapidly at increasing ζ, now large values of δ_g are connected to lower values of $\sum_{j=1}^{N}(x_{gk}(j)-\mu_j)/N$. Here we report even the results of the two-strip algorithms, and they are better than the four strip case. In general, the loss of the two strip COG could give incorrect results, the peak around zero can be very high and it drastically deforms φ. In this case, the noise washes away the peaks, and the noise reduction of the two strip algorithm gives a $\varphi(\varepsilon_2)$ more sensible to the asymmetry parameter δ_g than $\varphi(\varepsilon_4)$. The use of the two strip algorithms could be interesting in presence of high noise.

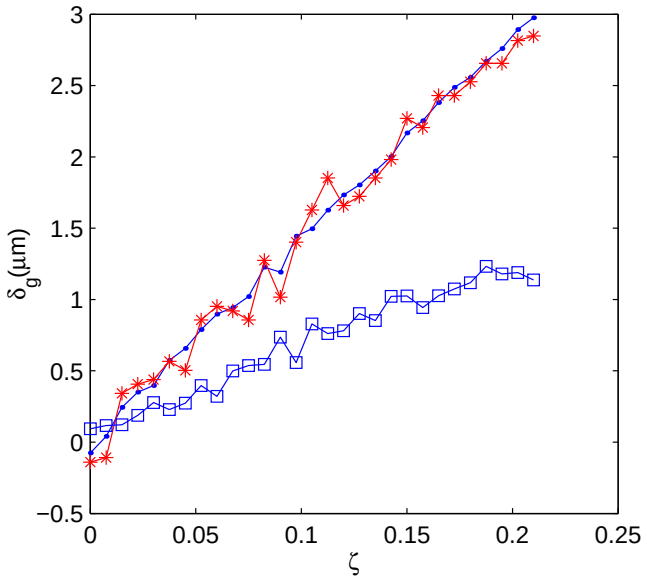

Figure 5. *Noiseless case. The blue dots indicate the results of equation 2.14.The red asterisks are the δ_g obtained by the minima of equation 3.9 with four-strip algorithm. The blue squares are the COG averages*

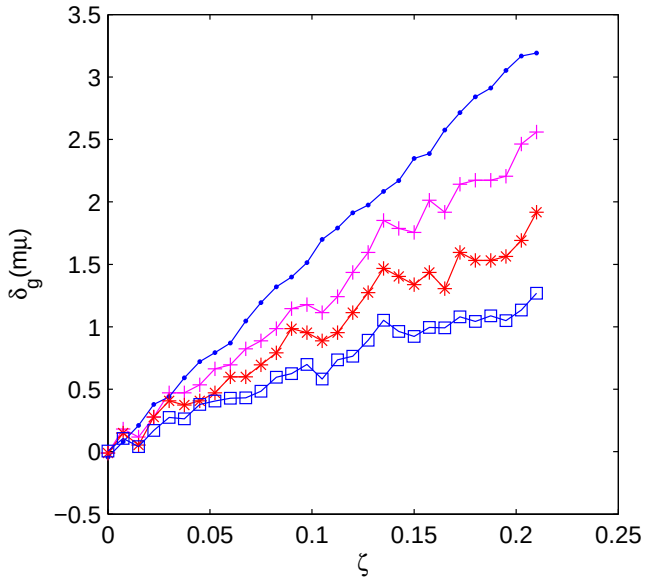

Figure 6. *The effect of the noise. The meanings of the symbols are that of figure 5. The magenta crosses indicate the δ_g obtained with the two-strip algorithm.*

4. Non orthogonal incidence and Lorentz angle

4.1 Asymmetry due to non orthogonal incidence

In the previous calculations, the orthogonality of the incoming particles was often recalled as a fundamental condition to access to the asymmetry of the response function. But, the effects of the deviations from the orthogonality must be explored to test the robustness of the algorithm. The β_n of equation 3.9 have terms $\Phi(-2\pi n)$ (FT of the true incoming $\varphi(x)$) in their definition 3.6, for the orthogonal incidence any $\Phi(-2\pi n)$ is real (and symmetric). An angular deviation θ ($\theta = 0$ for orthogonal incidence) from zero adds phase factors to the $\Phi(-2\pi n)$ and it introduces a large asymmetry in equation 3.9. Some plots of $\varphi(x)$ with $\theta \neq 0^o$ are reported in ref. [3]. For example, a value of $\theta = 0.2^o$ gives $\xi_m = 0.3\ \mu m$ for a symmetric response function (floating strip case). Thus, the asymmetry of the signal distribution, can easily mask the asymmetry of the response function. The θ data must have sufficient accuracy to detect small effects. In any case, the asymmetry induced by $\theta \neq 0$ changes its sign with the sign of θ and δ_g remains constant. So, for sufficiently small angles, where the total asymmetry is almost linear, the collection of data at various angles around $\theta = 0$ and the fit to the corresponding ξ_m with a low degree polynomial function can give a better value of δ_g.

To explore the variation of ξ_m from θ, we process the convolution $(\varphi * g_1)$ of our model [3] of $\varphi(x)$, with the machinery of equation 3.7. This is a very easy operation due the explicit FT expression of ref. [3]. The results are illustrated in figure 7 for the g_1 of floating strip sensors. A good linear relation is obtained for small θ values, this linearity is driven by two effects: a phase factor proportional to the angle in the model function, and the two copies of φ given by the two Dirac-delta of g_1. For comparison, in the normal strip case the absence of the two delta adds

non linear distortions. This linearity of ξ_m is saved (with a small reduction of the slope) in our reconstructed $\varphi(\overline{\varepsilon})$ and it is almost insensible to the noise.

The direct application of equation 3.7 on $\varphi * g_1$ gives ξ_m-values that depend very weakly on the asymmetry ζ due an almost complete cancelation of the first order terms. In any case, $\varphi * g_1$ is accessible only in the simulations and this cancelation is irrelevant in the data. On the contrary, the η-algorithms introduce phase factors proportional to δ_g in the FS-amplitudes of $\varphi(\overline{\varepsilon})$ as a global shift of the function. Thus, $\Omega(\xi)$ and equation 3.10 allow the extraction of δ_g from the data. After the proper δ_g-correction of the η-algorithm, $\Omega(\xi)$ gives a minimum for $\xi_m \approx 0$. The simulations

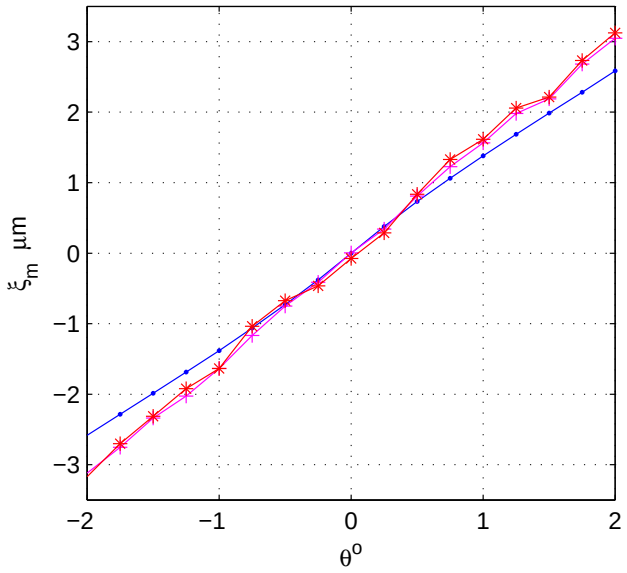

Figure 7. *Asymmetry $\zeta = 0$, floating strip sensors. Dotted line (blue) ξ_m on the convolution $(g_1 * \varphi)$ of the model signal distribution, asterisk line (red) ξ_m of $\varphi(\overline{\varepsilon}_4)$ and crosses line (magenta) is the ξ_m for the noiseless case.*

with an asymmetry $\zeta = 0.04$ are reported in figure 8 at different angles θ (step 0.25^o) of a floating strip sensor. As in figure 7, the ξ_m-values have a linear relation with the angles as in the symmetric case, but the line is shifted by $-1.14\mu m$ that is its crossing with the $\theta = 0$ line. This value is the systematic error of $\varepsilon_2(x_{g2})$ corrected with Δ_{02} for a symmetric response function, and, as expected, is constant in θ and equal to δ_g. The addition of the correction $-\delta_g$ to Δ_{02} completely eliminates the systematic error in $\varepsilon_2(x_{g2})$. The average of x_{g4} is different from zero at $\theta = 0$, signaling the asymmetry of the response function.

Similar results can be obtained for the normal strip case. The absence of the floating strip and the high noise make the plots of ξ_m to deviate from the good linearity of the floating case. Or better, the linear approximation has a restricted range of validity. As in figure 6, the asymmetry obtained from ξ_m is less than the right one and part of the systematic effect remains uncorrected. The ξ_m of $\varphi(\overline{\varepsilon}_2)$ gives a better estimation of δ_g than that of $\varphi(\overline{\varepsilon}_4)$, but it has a strong deviation from linearity. A fit with a low degree (3,4) polynomial function could be used. In any case, it is under study a more refined extraction of $\varphi(\overline{\varepsilon})$ from the data with a strong suppression of the noise distortion. Preliminary results [12] support a drastic improvement of the method

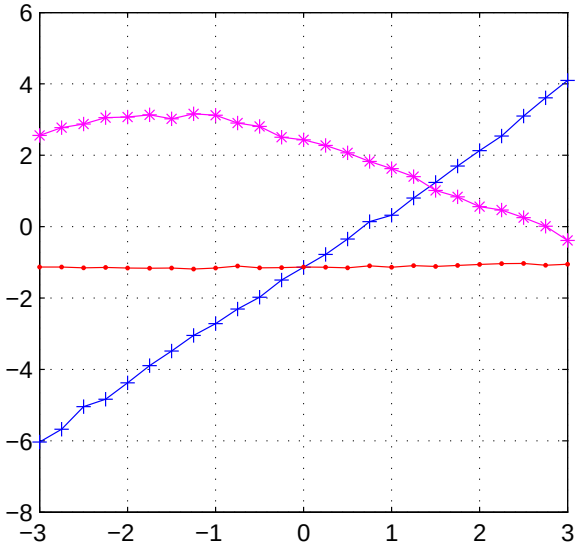

Figure 8. *Asymmetry $\zeta = 0.04$, floating strip sensor. Crosses line (blue) ξ_m of $\varphi(\overline{\varepsilon}_4)$, dotted line (red) systematic error of ε_2 without the correction δ_g and asterisks line (magenta) is the average of x_{g4}.*

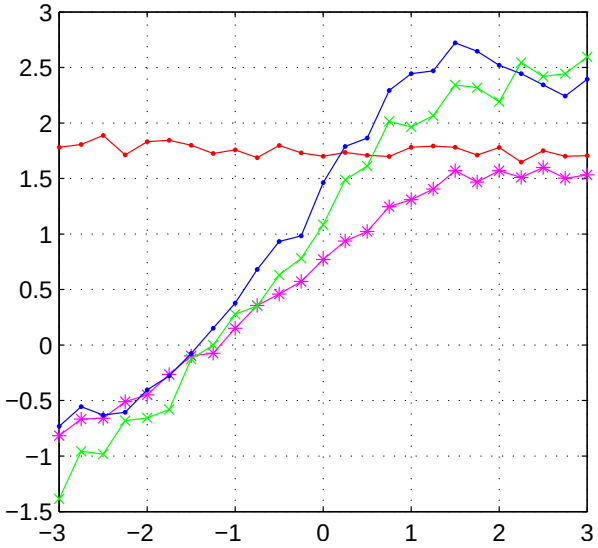

Figure 9. *Asymmetry $\zeta = 0.12$, normal strip sensor. Dot-blue line ξ_m of $\varphi(\overline{\varepsilon}_2)$, cross-green line ξ_m for $\varphi(\overline{\varepsilon}_4)$. Dot-Red line, systematic error of ε_2 without the correction δ_g, and asterisks-magenta line is the average of x_{g4}.*

4.2 Lorentz angle

The effect of the magnetic field on the particle-holes drift in a silicon detector is usually parameterized as a rotation of the particle path of an angle θ_L. The rotation is around an axis parallel to field containing the impact point. The effective COG of the track is shifted from the true one if the strip direction is non orthogonal to the field. The strips of the floating strip side of the PAMELA

detector are parallel to the magnetic field, and the assumed value of θ_L is 0.7^o. If the magnetic field has an effect similar to a rotation on the signal distribution, the present approach naturally measure θ_L. Usually, this measure is performed on the average length of the clusters produced by the MIP at various incidence angles. The minimum of the cluster size is at an incidence angle of $-\theta_L$ (in the geometry of ref. [3] where the impact point is always in the collection plane). At this angle, the apparent signal distribution is probably similar to that of an orthogonal incidence, or in any case it obtains its maximal symmetry.

The method to measure θ_L with the average cluster size has a low sensitivity just around the Lorentz angle. The data reported in ref. [13] shows clearly this limitation. It would be better to have a method with an high sensitivity just around θ_L. Our averages of $x_{g4,5}$ and ξ_m have the property to go to zero at $\theta = 0$ if the signal distribution and the response function are symmetric. Hence, in the case of symmetric condition around $\theta = -\theta_L$, the averages of $x_{g4,5}$ and ξ_m are able to measure θ_L. With the definition of θ_{eff}:

$$\tan(\theta_{eff}) = \tan(\theta) + \tan(\theta_L),$$

the COG algorithm sees a particle track with θ_{eff} bending angle, and its reconstruction has an effective shift of the true COG of:

$$\Delta_L = \frac{d}{2}\tan(\theta_L),$$

with d the depletion length of the detector (300 μm in our case of completely depleted sensors). The correction Δ_L must be subtracted by any reconstruction algorithm.

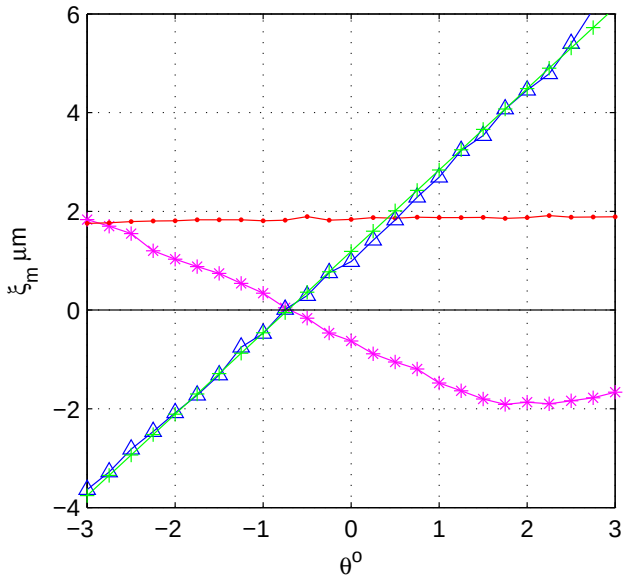

Figure 10. *Lorentz angle $\theta_L = 0.7^o$ symmetric floating strip sensor. Triangles-blue line ξ_m of $\varphi(\overline{\varepsilon}_4)$. Crossed-green line: linear interpolation of ξ_m . Dot-red line systematic error of ε_2 without the correction Δ_L, and asterisks-magenta line is the average of x_{g4}.*

Figure 10 illustrates the sensitivity of ξ_m and the of average of x_{g4} to $\theta_L \neq 0$, each one crosses the $\theta = 0$ line around -0.7^o (ξ_m at -0.72^o and x_{g4} at -0.70^o). Here the detector is perfectly

symmetric, thus, the average of x_{g4} is an easy and sensible tool to extract θ_L. The asymmetry parameter ξ_m is equally sensible, but more complex to calculate. It is clear that the symmetry condition can be verified in the detector without magnetic field, and the average of x_{g4} must be zero for $\theta = 0$. In the case of an asymmetric response function one has to resort to ξ_m. For its structure ξ_m is produced by two independent effects: the asymmetry of the response function and the effective deviation from orthogonality. The asymmetry of the response function δ_g must be measured without the magnetic field and the $x_{g4,5}$ corrected accordingly. With the corrected $x_{g4,5}$, ξ_m goes again to zero for $\theta = 0$. The correction δ_g is constant with θ, thus, the addition of the magnetic field gives $\xi_m = 0$ at $\theta = -\theta_L$. The presence of the asymmetry $\delta_g \neq 0$ drastically modifies the averages of x_{g4} or x_{g5}, and they never go to zero for $\theta = 0$, or $\theta = -\theta_L$ with the magnetic field and are not usable to measure θ_L.

The combined effect of the Lorentz angle and the asymmetry δ_g is illustrated in figure 11. Here, a simulation of the floating strip sensor with the asymmetry of figure 8 and a θ_L rotation, is elaborate as in figure 10.

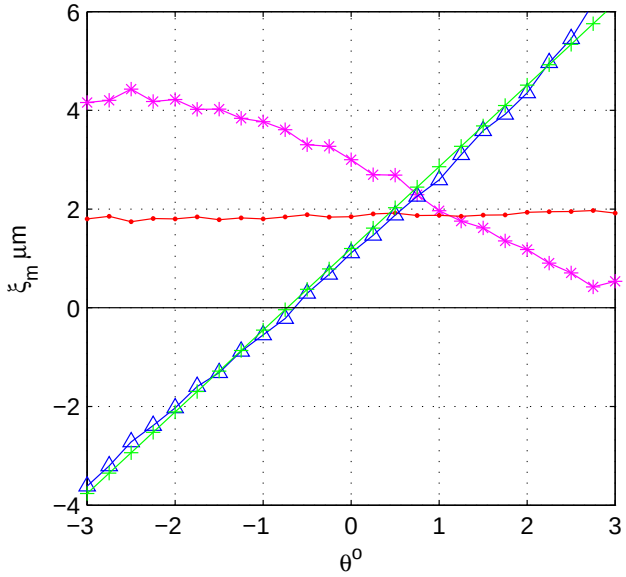

Figure 11. *Lorentz angle $\theta_L = 0.7^o$ asymmetric floating strip sensor $\zeta = 0.04$. Triangles-blue line ξ_m of $\varphi(\overline{\varepsilon}_4)$. Cross-green line: linear interpolation of ξ_m . Dot-red line systematic error of ε_2 without the correction Δ_L, and asterisks-magenta line is the average of $x_{g4} - \delta_g$.*

Now, figure 11 shows that ξ_m, corrected with δ_g continues to cross the zero line at $\theta_L = -0.7^o$. The corrected average of x_{g4} does not cross the zero line at $\theta_L = -0.7^o$ and its use as an estimator of θ_L is destroyed by $\delta_g \neq 0$. An interesting property of ξ_m is its sensitivity to two types of asymmetry that combine in a non interfering way. The correction of $\delta_g \neq 0$ can be implemented in x_{g4} at the beginning of the calculation of ξ_m or implemented at the end (subtracting its value from ξ_m). These two different procedures give identical results. This property resembles a linear combination of effects.

Similar analysis performed on the normal strip sensors gives analog results. The quality of the

θ_L determination has a similar precision, its resolution is better than that of δ_g.

5. Conclusions

The properties of the COG algorithms are able to access at a very detailed aspects of the detector: the COG position of the response function and the Lorentz angle. The direct measurement is sufficiently complex and could be unnecessary in many typical case. This extraction can estimate these parameters from the data acquired in standard test beam (or in a running experiment), with a simpler requirement of precise angular positioning of the detector. The noise introduces perturbation, but a strong relation to the asymmetry is saved even in the worst case. The Lorentz angle determination shows a modest sensitivity to the noise.

The present procedure is able to separate the intrinsic asymmetry of the $\varphi(\varepsilon)$ and the induced asymmetry due to incorrect initial conditions. The minimal asymmetry should be the intrinsic one, but it is conceptually difficult to separate the two. In spite of this, the simulations show an excellent ability to detect δ_g in the noiseless cases, giving to the phase shifts of equation 3.10 a robust meaning in the explored range of asymmetry. The noise modifies this picture adding a blurring in the reconstructions that perturbs the efficacy of equation 3.10. But, the moderate noise of the floating strip side has a negligible effect on δ_g. In the simulations, the x_{g4} has a RMS of $4.2\mu m$ on a strip pitch of $51\mu m$. For the normal strips, the noise is drastically higher (a RMS of $10.6\mu m$ on a strip pitch of $63\mu m$) and δ_g estimation appreciably degrades. The noise tends to mask the effect of the asymmetry adding deformations that round $\varphi(x)$ with a decreasing of the resulting δ_g.

The indicator of a non zero δ_g is the average of x_{gk} at orthogonal incidence. In the two cases we explored, this average has a quite different relation to the asymmetry. In the first case, to a large x_{gk}-averages corresponds a small asymmetry, the reverse in the second case. Equation 3.1, as in the example of figure 1, allows a visual inspection of $\varphi(x)$. For normal strips, the noise in the x_{g4}-algorithm masks almost completely the asymmetry, but the two strip algorithm is able to give interesting results.

The asymmetries we consider have their principal effect on the central strip. The capacitive coupling introduces long range interactions in the nearby strips, and these interactions can be asymmetric. The x_{gk}-averages are sensible to very small effects and they may signal even long range asymmetries. Equation 3.1 is not fit to handle these effects, it overlaps the tails of the $\varphi(x)$ outside a strip range creating fake distortions. Assembly of strips must be explored if an indication of these long range effects is acquired.

The robustness of the approach is tested at non orthogonal incidence angle. The parameter ξ_m shows a surprising strict linear behavior, in the case of floating strip sensor, that allows an increase of precision with a linear interpolation of the data. For the normal strip case, appreciable deviation from linearity are observed, but, even in this case an interpolation with a low degree polynomial has beneficial effects on the δ_g determination.

The simulations at non orthogonal incidence suggest that the approach can be used for the Lorentz angle determination. The approximation of the magnetic field effect as an effective rotation of the reference system is probably very rough, in any case ξ_m is able to detect the angle of maximal symmetry with an excellent precision. In the case of $\delta_g = 0$ other simpler indicators has a comparable sensitivity to the maximal symmetry: the averages of x_{g4} and of x_{g5} cross the $\theta = 0$

line at the maximal symmetry. These indicators become useless in presence of small $\delta_g \neq 0$. On the contrary ξ_m saves its efficiency to detect the maximal symmetry even in presence of $\delta_g \neq 0$. With a first set of measurements without the magnetic field, δ_g can be measured and this correction must be implemented in the ξ_m calculation on the data with the magnetic field/effective rotation. Now ξ_m crosses the $\theta = 0$ line at $-\theta_L$ as expected (with our angle definitions). The two effects of the effective rotation and $\delta_g \neq 0$ look to combine in an almost independent way. In fact, the correction δ_g can be used to correct x_{g4} or x_{g5} before calculating ξ_m, or the correction δ_g can be applied directly at the end of the ξ_m determination with identical results.

All these simulations assume small values of δ_g and θ_L. It is evident that the explored values of δ_g are larger than these we can expect from the detectors; the limitation to θ_L are easily overcome working around the expected θ_L to have an its precision determination where the standard methods have a low sensibility.

References

[1] G. Landi, *Properties of the center of gravity as an algorithm for position measurements,* *Nucl. Instrum. and Meth. A* 485 (2002) 698.

[2] G. Landi, *Properties of the center of gravity as an algorithm for position measurements: two-dimensional geometry,* *Nucl. Instrum. and Meth. A* 497 (2003) 511.

[3] G. Landi, *Problems of position reconstruction in silicon microstrip detectors,* *Nucl. Instr. and Meth. A* 554 (2005) 226.

[4] E. Belau et al., *Charge collection in silicon strip detector,* *Nucl. Instrum. and Meth. A* 214 (1983) 253.

[5] P. Picozza et al. *PAMELA-A Payload for Matter Antmatter Exploration and Light-nuclei Astrophysics* *Astropart. Phys.* 27 (2007) 296 [astro-ph/0608697]

[6] O. Adriani et al. *"In-flight performance of the PAMELA magnetic spectrometer",* 16^{th} *International Workshop on Vertex Detectors* September 2007 NY. USA. PoS(Vertex 2007)048

[7] G. Batignani et al., *Double sided read out silicon strip detectors for the ALEPH minivertex,* *Nucl. Instrum. and Meth. A* 277 (1989) 147.

[8] O. Adriani, *et al.*, [L3 SMD Collaboration] *The New double sided silicon microvertex detector for the L3 experiment. Nucl. Instrum. Meth. A* **348** (1994) 431.

[9] R.N. Bracewell, *"The Fourier Transform and Its Application"* (McGraw-Hill, New York, NY, 1986).

[10] H. Dym, H.P. McKean, *"Fourier Series and Integrals"* (Academic Press, London, 1972).

[11] I. Abt et al., *Characterization of silicon microstrip detectors using an infrared laser system,* *Nucl. Instrum. and Meth. A* 423 (1999) 303.

[12] G.E. Landi, *"Figure restorations"*. UBICA Reports 2011

[13] CMS Collaboration, "Commissioning and performance of the CMS silicon tracker with cosmic ray muons" 2010 *JINST* **5** T03008